Inorganica Chimica Acta 414 (2014) 234–239

Contents lists available at ScienceDirect

Inorganica Chimica Acta

journal homepage: www.elsevier.com/locate/ica

# An unexpected electro-luminescent properties of scandium(III) heteroaromatic 1,3-diketonate complex

Ilya Taydakov [a,*], Andrey Vaschenko [a], Yuri Strelenko [b], Alexey Vitukhnovsky [a]

[a] S.I. Vavilov Luminescence Laboratory, P.N. Lebedev Physical Institute, Russian Academy of Sciences, Leninsky Prospect 53, 119991 Moscow, Russian Federation
[b] N.D. Zelinsky Institute of Organic Chemistry, Russian Academy of Sciences, Leninsky Prospect 47 , 119991 Moscow, Russian Federation

ARTICLE INFO

*Article history:*
Received 4 November 2013
Received in revised form 4 February 2014
Accepted 10 February 2014
Available online 18 February 2014

*Keywords:*
Scandium(III) complexes
Electroluminescence
OLED
$^{45}$Sc NMR

ABSTRACT

A novel complex of Sc(III) with pyrazole substituted 1,3-diketone (1,3-bis(1,3-dimethyl-1*H*-pyrazol-4-yl)-1,3-propanedione) was synthesized and characterized by X-ray diffraction, nanotechnology-assisted laser desorption/ionisation time-of-flight mass spectroscopy (NALDI-TOF-MS) and NMR spectroscopy, including $^{45}$Sc NMR. The first sample of organic light-emitting diode (OLED) based on heteroaromatic Sc(III) 1,3-diketonate as an active layer was fabricated and tested. The maximum intensity of yellowish-green electroluminescence (530–560 nm) was equal to 40 cd/m$^2$ and turn-on voltage was about 4.5 V. Further device modification and ligand structure optimization can lead to a better performance of such materials for OLEDs.



## 1. Introduction

Since Kido and co-workers reported [1] about the first electroluminescent device based on simple terbium complex Tb(acac)$_3$ in 1990, much efforts were made to develop effective lanthanide-base light emitters for OLED during the last two decades. Complexes of all lanthanides (except for La, Pm, Gd and Lu) were tested for this application, and the best results were obtained for terbium (green), europium and samarium (red–orange), ytterbium and erbium (near infra-red spectral region) compounds. These results are summarized in several comprehensive reviews [2–5].

The simplified scheme of electroluminescence of lanthanide complexes involves excitation of triplet and singlet levels of organic ligand by excitons and succeeding energy transfer to resonance f-levels of $Ln^{3+}$ ion by dipole–dipole Föster mechanism [6].

The $f^* \rightarrow f$ transitions are resulted to the light emission, usually in a narrow spectral range. The emission spectrum weakly depends on the nature of ligand. Of course, this transfer may be accompanied by a number of nonradiative processes both ligand and central ion, and intermolecular energy conversion. All these ways of relaxation generally decrease the efficiency of the metal-centered light generation.

Moreover, light may be emitted by $S^1 \rightarrow S^0$ (fluorescence) and $T^1 \rightarrow S^0$ (phosphorescence) relaxation pathways directly in the ligand. The triplet–singlet relaxation is spin forbidden, but this route can be realized in the presence of heavy atoms due to spin–orbital interactions. Although this way (ligand-centered luminescence) is not typical for lanthanide complexes, it becomes the main route for high-luminescent complexes of non-transitions elements such as tris(8-hydroxyquinolinato)aluminum (Alq$_3$). Up to now Alq$_3$ is one of the best green luminescent and electron-transport material [7].

Scandium(III) has no f-electrons and electron configurations of $Sc^{3+}$ and $Al^{3+}$ ions are similar. Probably this fact was a starting point to test Sc(III) complexes as new electroluminescent materials. It was Bochkarev who firstly reported [8] that Tris(8-hydroxyquinolinato)scandium was better electroluminescent material than Alq$_3$. Later some promising materials based on O,N- or S,N-donor ligands [9] were developed by researches of Bochkarev's group. Scandium-based materials demonstrate bright yellow, green or white ligand-centered electroluminescence and good electrical conductivity .

To our best knowledge, Sc(III) complexes based on 1,3-diketonato ligands were early not tested as electroluminescent materials. Yttrium(III) 1,3-diketonates were reported [10] as dopants for isostructural Eu(III) complexes. They improved conductivity but did not affect on the spectral characteristic of the emission.

A number of complexes with other rare earths ions and pyrazole substituted 1,3-diketones obtained by us were described and discussed early [11].

Due to our continuous interest in synthesis and application of novel 1,3-diketonato ligands bearing pyrazole moiety, here we wish to report about synthesis and electroluminescent properties of scandium(III) tris(1,3-bis(1,3-dimethyl-1*H*-pyrazol-4-yl)-1,3-propanedionate).

* Corresponding author. Tel.: +7 916 1381665.
*E-mail address:* taidakov@gmail.com (I. Taydakov).

http://dx.doi.org/10.1016/j.ica.2014.02.013
0020-1693/

## 2. Experimental

### 2.1. General information

Ligand was synthesized by the previously described method [12]. All other reagents were purchased from Aldrich and used without further purification. Elemental analysis was performed on the Elementar CHNO(S) analyzer.

Special reagents and ITO coated glass slides (resistance 10–15 Ω/sq) for OLED fabrication were purchased from Lumtec Corp. (Taiwan).

UV–Vis absorption spectra were recorded on the Perkin-Elmer Lambda 45 instrument. Luminescent spectra were obtained on the Perkin-Elmer SL-45 spectrofluorimeter equipped with a fiber optics probe and xenon flash lamp.

Nanotechnology-assisted laser desorption/ionisation time-of-flight mass spectrometry spectra (NALDI-TOF-MS) were obtained on the Bruker Autoflex Speed instrument equipped with nitrogen pulse laser (337 nm). Samples in form of 2 mg/mL solutions in EtOH were dropped on the surface of the nano-structured target (Bruker MSP 96 NALDI target) and dried. Spectra were collected in a positive mode.

TGA-DSC analysis was performed on the Netzsch STA 449C instrument in $Al_2O_3$ crucibles in the temperature range 20–900 °C (293–1173 K). Heating rate was 10 K/min, mixture of air (40 mL/min) and Ar (20 mL/min) was used as an oxidation environment.

FTIR spectra were obtained on the Bruker Vector 22 instrument in KBr pellets.

NMR study was performed in DMSO-$d_6$ solutions at 298 K on the Bruker DXR-500 instrument operating at 500.1, 125.8 and 121.5 MHz for $^1$H, $^{13}$C and $^{45}$Sc nucleus respectively. TMS ($\delta$ = 0.00 ppm) was used for $^1$H and $^{13}$C NMR measurements as a internal standard, and 1.5 M solution of $Sc(NO_3)_3 * 5H_2O$ in $D_2O$ at pH 1 was used as external standard ($\delta$ = 0.0 ppm) [13] for $^{45}$Sc NMR measurements.

Current–voltage–brightness characteristics of the organic LEDs were measured on the Keithley (Keithley, USA) digital multimeter and the TKA (Russia) luminance meter. The electroluminescence and photoluminescence spectra were measured on the multi-channel spectrometer S2000 (Ocean Optics, USA).

### 2.2. Synthesis and characterization of complex **2** ($ScL_3$)

Solution of $ScCl_3$ was prepared by treatment of $Sc_2O_3$ (1.0 g, 7.25 mmol) with pure conc. HCl, evaporation of the reaction mass to dryness and dissolution of the residue in deionized water in a volumetric flask. Overall volume was brought to 10 mL.

In 7 mL of ethanol 0.575 g (2.17 mmol) of HL was dissolved. To this solution 0.5 mL (0.725 mmol) of $ScCl_3$ solution was added with stirring and pH was adjusted to 9 by the carefully addition of aqueous ammonia. The reaction mixture was held at 50 °C for 2 h, cooled and the precipitate was filtered and washed successively by small portions of water, 30% aqueous ethanol and ether and finally dried at $10^{-2}$ Torr and 45 °C to a constant weight. Yield of the white crystalline powder is 0.27 g (53%).

Analytical sample was recrystallized from DMSO–$CH_2Cl_2$ mixture, washed with $CH_2Cl_2$ and dried to a constant weight under the diminished pressure ($1 \times 10^{-2}$ Torr).

Elemental analysis: *Anal.* Calc. for $C_{39}H_{45}N_{12}O_6Sc$: C, 56.93; H, 5.51; N, 20.43; Sc, 5.46. Found: C, 57.07; H, 5.79; N, 20.67, Sc, 5.51%.

$^1$H NMR (DMSO-$d_6$) $\delta$ (ppm): 7.95 (br. s, 6H, Pyr–H), 5.9 (s, 3H, C═CH), 3.70 (s, 18H, N–$CH_3$), 2.30 (s, 18H, $CH_3$).

$^{13}$C NMR (DMSO-$d_6$) $\delta$ (ppm): 177.83 (C═O), 149.96 ($C(3)_{Pyr}$), 132.09 ($C(5)_{Pyr}$), 126.61 ($C(4)_{Pyr}$), 95.54 (CH═), 38.19 (N–$CH_3$), 13.73 ($CH_3$).

$^{45}$Sc NMR (DMSO-$d_6$) $\delta$ (ppm): 96.9.

IR $\nu$($cm^{-1}$): 1657, 1540, 1465.

### 2.3. X-ray crystal data

Single crystals of **2a** or **2b** suitable for X-ray diffraction were obtained by slow diffusion of MeCN vapor into saturated solution of **2** in DMSO or DMSO–EtOH (1/1 by volume) at the room temperature. Crystals are not stable in air at the room temperature and lose the solvent with crystal degeneration easily.

Two different crystal modifications (solvatomorphs [14]) of complex **2** were obtained from different solvents. Rhombohedral crystals of **2** * 3MeCN solvate (**2a**) were obtained from MeCN–DMSO mixture while monoclinic crystals of 2 * MeCN * EtOH (**2b**) were formed in the presence of EtOH. All diffraction data were collected on the Bruker SMART APEX II CCD diffractometer [$\lambda$(Mo K$\alpha$) = 0.071072 nm, $\omega$-scans]. The substantial redundancy in data allows empirical absorption correction to be performed with SADABS [15,16], using multiple measurements of equivalent reflections.

The structures were solved by a direct method and refined by the full-matrix least-squares technique against $F^2$ in the anisotropic approximation for all non-hydrogen atoms. In the crystal of solvate **2b** for the disordered ligand (see Fig. 1 in Supplementary) the refinement was performed with additional constraints on C–C, C–O and C–N bond lengths and anisotropic displacement parameters of corresponding atoms.

The positions of hydrogen atoms were calculated and refined with the riding model in the isotropic approximation. In crystals of solvate **2b** the analysis of the Fourier electron density synthesis has revealed that solvate molecules are strongly disordered and with high probability the observed electron density maxima can be attributed to superposition of ethanol and acetonitrile. We failed to establish appropriate model for refining of the above residual electron density corresponding to this molecules. That is why we had to exclude unresolved solvents by means of SQUEEZE procedure [17]. Taking into account that disordered ligand predominantly forms intermolecular interactions with superimposed solvate it is reasonable to propose that observed disorder of the latter is the consequence of intermolecular interactions.

All calculations were performed with the SHELXTL software package [16].

### 2.4. OLED device fabrication

In this study a series of multilayer OLED structures with the $ScL_3$ as an emissive layer was prepared. Conductive layer – PEDOT:PSS (poly-ethylene dioxythiophene:poly-styrenosulphonate) and a hole transport layer – TPD (*N*,*N*-diphenyl-*N*,*N*-bi(3-methylphenyl)-[1,1′-diphenyl]-4,4′-diamine) were deposited by the solution spin-coating technique. The electron transporter layer – TAZ (3-(4-biphenyl)-4-phenyl-5-tert-butylphenyl-1,2,4-triazole), $Alq_3$

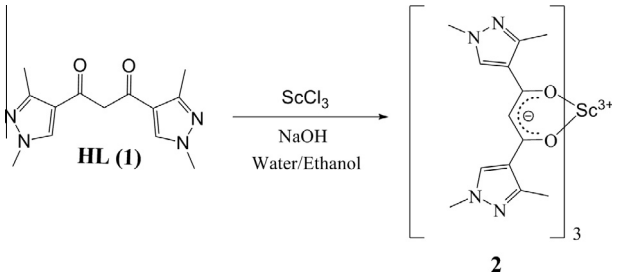


**Fig. 1.** Synthesis of complex **2**.

(Tris(8-hydroxy-quinolinato)aluminum) and complex **2** were deposited by thermal evaporation.

The evaporation was performed at $10^{-5}$ mbar using resistively heated tungsten boats. Deposition rate was kept at 0.05–0.2 nm/s and controlled by the Inficon IC-6000a calibrated microquartz deposition controller. Aluminum cathode was deposited at $5 \times 10^{-6}$ mbar at a rate 1–2 nm/s. The emitting area was about 10 $mm^2$.

## 3. Results and discussion

### 3.1. Synthesis of complex *2* ($ScL_3$)

Complex **2** was synthesized according to the following scheme (Fig. 1):

Complex **2** had low solubility in common solvents such as ethanol or dichloromethane and was purified by successively washing with ethanol and water from starting materials and other impurities. It can be additionally recrystallized from large amount of hot EtOH, but solvent vapor diffusion method is better one to obtain good crystals.

### 3.2. Crystal structures of *2a* and *2b*

Crystal data and structure refinement parameters for **2a** and **2b** are summarized in Table 1.

The coordination polyhedron for sixfold coordinated Sc atom in both solvatemorphs **2a** and **2b** is a distorted trigonal antiprism. In the crystal of **2a** molecule occupies the 3-fold axis while **2b** all atoms are located in general position. The Sc–O bond distances in **2a** and **2b** (for ordered ligands) vary in the narrow range 2.078(1)–2.095(1) Å and almost equal to those found out in the $Sc(tfacac)_3$ (Htfacac – trifluoroacetylacetone) complex [18]. The analysis of crystal packing have revealed that all intermolecular contacts corresponds to the normal Van-der-Waals interactions of C–H···π, C–H···N and H···H types (see Figs. 2 and 3 in Supplementary) The molecular structure of **2a** is shown in Fig 2.

### 3.3. NALDI-MS and TGA studies

Application of mass-spectroscopy for the identification of complexes is very attractive task. We have systematically studied an optimal conditions for MS determination of pyrazole substituted 1,3-diketonates of rare earths [19]. Unfortunately, most of these compounds are unstable under laser irradiation even in the presence of different matrixes. More stable and predictable results were obtained without matrix. Stainless steel (standard type) or nano-structured targets are both suitable for the analysis, but better spectra were obtained with the last one.

**Table 1**
Crystal data and structure refinement parameters for **2a** and **2b**.

| | 2a | 2b |
|---|---|---|
| Empirical formula | $C_{45}H_{54}N_{15}O_6Sc$ | $C_{42}H_{54}N_{13}O_7Sc$ |
| Formula weight | 945.99 | 897.94 |
| $T$ (K) | 100 | 100 |
| Crystal system | rhombohedral | monoclinic |
| Space group | $R\bar{3}$ | $P2_1/n$ |
| $Z(Z')$ | 3(1/3) | 4 |
| $a$ (Å) | 19.1881(14) | 11.8292(6) |
| $b$ (Å) | 19.1881(14) | 17.3915(9) |
| $c$ (Å) | 11.1360(8) | 21.7841(11) |
| $\beta$ (°) | 90.00 | 93.0564(11) |
| $V$ (Å$^3$) | 3550.8(4) | 4475.2(4) |
| $D_{calc}$ (g cm$^{-3}$) | 1.327 | 1.333 |
| $\mu$ (cm$^{-1}$) | 2.2 | 2.29 |
| $F(000)$ | 1494 | 1896 |
| $2\theta$ maximum (°) | 57 | 58 |
| Reflections collected ($R_{int}$) | 6836 (0.0261) | 35083 (0.0355) |
| Independent reflections | 3873 | 11875 |
| Observed reflections with $I > 2\sigma(I)$ | 3406 | 8578 |
| Number of parameters/restraints | 208/1 | 588/141 |
| $R_1$ | 0.0327 | 0.0553 |
| $wR_2$ | 0.0771 | 0.1502 |
| Goodness of fit (GOF) on $F^2$ | 1.034 | 1.056 |
| Largest difference peak and hole, e (nm)$^{-4}$ | 0.287/−0.265 | 1.259/−0.453 |

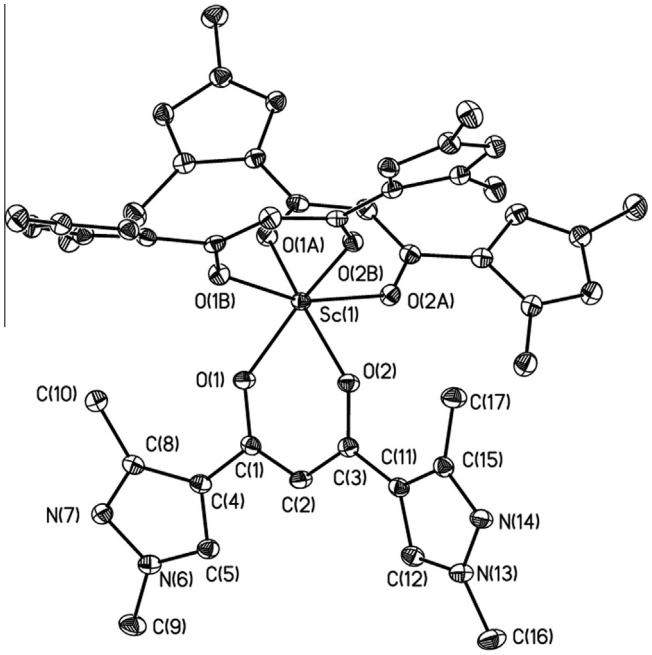


**Fig. 2.** The general view of complex **2a** in representation of atoms by thermal ellipsoids ($p$ = 50%). Hydrogen atoms have been omitted for clarity.

Primary ion formation mechanisms in NALDI method are differ from electron impact (EI) ionization. Two main processes are predominated – (i) proton transfer, that lead to formation of protonated ions such as $[M+H]^+$ or (ii) cationization in which ions such as $[M+Cat]^+$ (Cat = $NH_4^+$, $Na^+$, $K^+$, etc.) are formed. Specific pathway of the ionization is thermodynamically and kinetically controlled, but formation of complex ions rather then simple molecular ion is a common phenomenon in NALDI (and MALDI) mass spectrometry [20].

NALDI spectrum of complex **2** is relatively simple. The most intense signal ($m/z$ = 536.788, 100%) was attributed to $[ScL_2]^+$ ion. Other signal with $m/z$ = 846.101 (4.5%) was referred to $[ScL_3+Na]^+$ fragment. The formation of more heavy ions was not observed under these conditions. No simple molecular ion was detected in the spectrum.

The first sharp endothermic peak on TGA-DSC curve at 297.3 °C corresponds to the melting of complex **2**. Exothermic decomposition of the compound **2** started at 419.5 °C and finished at 725.1 °C. Weight of the residue ($Sc_2O_3$) was 7.89% at 900 °C (theoretical mass 8.38%).

### 3.4. NMR studies

High sensitivity (0.3 relative to $^1H$) of the $^{45}Sc$ nuclei and moderate quadrupole moment ($-0.22 \times 10^{-28}$ m$^2$) make it potentially possible to use $^{45}Sc$ NMR for the investigation of its coordination compounds.

Since coordination bonds in the $ScL_3$ are considerably covalent, no ligand exchange was obtained even in the DMSO solutions. Another favorable factor is a relatively high symmetry of complex **2** in the solution. But actually we could not obtain sufficiently narrow

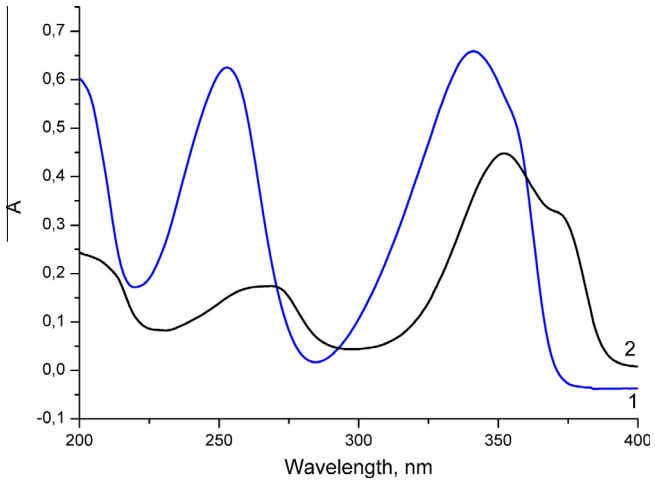


**Fig. 3.** UV–Vis absorption spectra of HL (1, blue line) and complex **2** (2, black line) in acetonitrile. (For interpretation of the references to colour in this figure legend, the reader is referred to the web version of this article.)

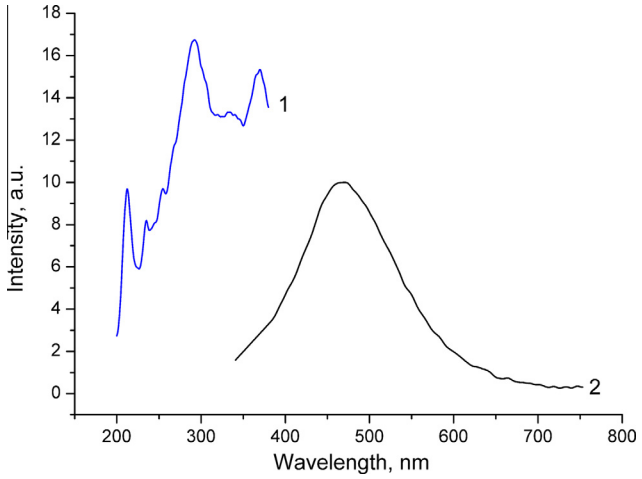


**Fig. 4.** The excitation spectrum (1, blue line) of $ScL_3$ crystal ($\lambda_{em}$ = 467 nm) and normalized emission ($\lambda_{ex}$ = 337 nm) spectra (2, black line). (For interpretation of the references to colour in this figure legend, the reader is referred to the web version of this article.)

signals. After Lorentzian approximation by the Bruker TopSpin software the width of the signal at the half of height was estimated as 4440 ± 26 Hz.

The chemical shift of the $^{45}Sc$ NMR signal (96.9 ± 0.1 ppm) for the compound **2** was measured relatively to 1.5 M $Sc(NO_3)_3$ ($\delta$ = 0.0) aqueous solution. Practically the same value (89 ppm) was reported [13] earlier for $Sc(acac)_3$ in benzene or $CHCl_3$ solutions.

Therefore one can assume that the new ligand **1** is slightly stronger electron acceptor than acetylacetone (Hacac). Unfortunately, $Sc(acac)_3$ seems to be the only one complex with 1,3-diketone for which $^{45}Sc$ NMR chemical shift was reported previously, so there are no enough data for any reliable correlations.

The $^{1}H$ and $^{13}C$ NMR spectra were measured by a common way and fully matched to the structure of the complex $ScL_3$.

### 3.5. Photophysical study of *2*

The UV–Vis absorption spectra of **HL** (1) and complex **2** (2) in acetonitrile (solutions with concentrations of $4.4 \times 10^{-5}$ and $1.7 \times 10^{-5}$ M, respectively were used) are shown in Fig. 3.

Complex **2** is demonstrated high UV-light absorption in the wide spectral range (200–380 nm). Absorption maxima in $ScL_3$ spectrum are red-shifted relative to the spectrum of free ligand and characterized by high extinction coefficient (26470 at 350 nm).

The excitation spectrum (**1**) of $ScL_3$ crystal ($\lambda_{em}$ = 467 nm) and the emission spectra of **2** in crystals (**2**) are shown in Fig. 4.

As far as $Sc^{3+}$ has no f-electrons, only the ligand-centered luminescence can be observed. Weak greenish-blue emission is characterized by relatively wide band of molecular luminescence with maximum at 467 nm. Emission spectra of bulk crystalline material and thin film, deposited by high vacuum evaporation on glass slide (see below, Fig. 6), are virtually identical. One can assume that complex **2** is not decomposed during high vacuum deposition. No phosphorescence was detected at the room temperature.

### 3.6. Electroluminescent properties of *2*

Structures of three different multilayer devices that were fabricated (designated as devices 1–3), and chemical structures of the materials used in the present study are shown in Fig. 5.

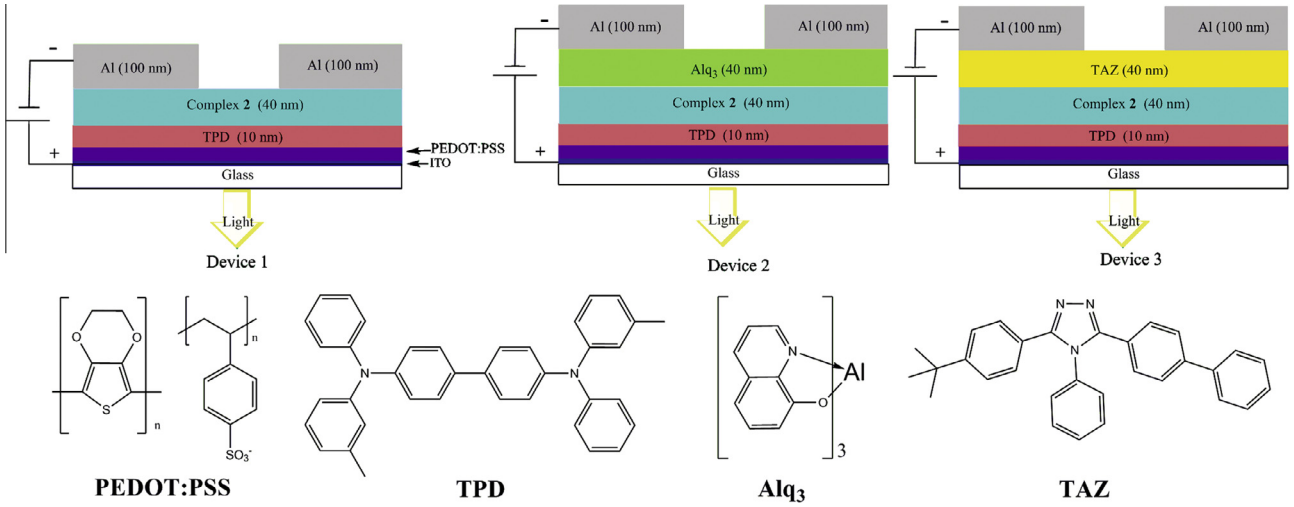


**Fig. 5.** Structures of OLEDs (devices 1–3).

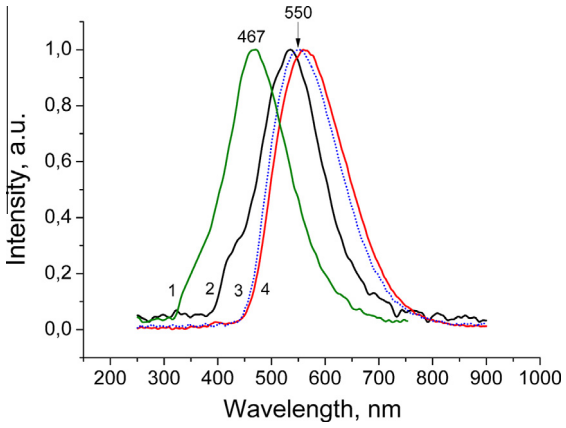


**Fig. 6.** PL spectrum of $ScL_3$ film (1, green line) and EL spectra of devices 1 (2, black line), 2 (3, blue dotted line) and 3 (4, red line). (For interpretation of the references to colour in this figure legend, the reader is referred to the web version of this article.)

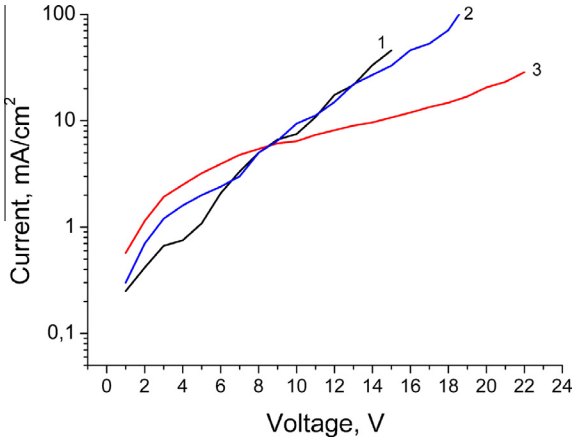


**Fig. 7.** Volt–current dependencies for devices 1 (1, black line), 2 (2, blue line) and 3 (3, red line). (For interpretation of the references to colour in this figure legend, the reader is referred to the web version of this article.)

Volt–current dependencies and electroluminescence (EL) spectra of OLEDs structures with $ScL_3$ as an emitting layer along with photoluminescence (PL) spectra of **2** are shown in Fig. 6.

The devices exhibited bright yellowish luminance with the maximum brightness of about 40 cd/m$^2$. The turn on voltage was about 4.2–5.0 V indicating quite good agreement of HOMO and LUMO levels of used organic materials. The EL peak wavelength of $ScL_3$ was significantly shifted to 532 nm (device 1), 551 nm (device 2) and 563 nm (device 3) with respect to PL peak at 467 nm, which may be the result of exciplex formation at the TPD/$ScL_3$, $Alq_3$/$ScL_3$ or TAZ/$ScL_3$ surfaces.

We also found no dependence of wavelength of EL peak on voltage applied to OLED, This indicates that the Stark effect could not be responsible for observed spectral shift. Moreover we found a slight broadening of emission spectra of 155 nm of devices 2 and 3 with respect to 140 nm in photoluminescence spectra of device 1, that may also be attributed to exciplex formation in devices 2 and 3.

It is possible that $Alq_3$ is responsible for some part of EL in device 2 as $Alq_3$ PL peak is in the same spectral region (530–540 nm). Although it is clear that we observed only EL of complex **2** in devices 1 and 3 because PL emissions peaks of TPD and TAZ (398 nm and 370 nm respectively) are far from spectral peaks of acquired OLED devices.

It is worth noting that volt–current dependencies (Fig. 7) of devices 1 and 2 are similar while device 3 exhibited more sloping characteristic. This may be attributed to the better hole blocking ability of TAZ than $Alq_3$.

## 4. Conclusion

In summary, scandium(III) complex with novel ligand 1,3-bis(1,3-dimethyl-1*H*-pyrazol-4-yl)-1,3-propanedionate was synthesized and characterized by X-ray single crystal diffraction, elemental analysis, NALDI-TOF-MS and NMR on $^1$H, $^{13}$C and $^{45}$Sc nucleus. It was demonstrated that this compound formed solvates while being crystallized from mixed solvents (DMSO–EtOH–MeCN).

The first sample of OLED device with heteroaromatic Sc(III) 1,3-diketonato complex as the light-emitting layer was fabricated by vacuum deposition/spin coating technique and successfully tested. This OLED emits yellowish light (maximum at 530–560 nm) with 40 cd/m$^2$ overall brightness.

The possible mechanism of PL can be explained by emission from $\pi^*$ to $\pi$ states of organic ligand. Thus, 1,3-diketonates of Sc(III) with heteroaromatic or aromatic ligands are promising candidates for the fabrication of multilayer electro-optical devices. Further device modification and optimization can lead to a better performance of this material in OLEDs.

## Acknowledgments

We are grateful to Prof. Konstantin Lyssenko (X-Ray Structural Centre Chemistry and Material Sciences Division of A.N.Nesmeyanov Institute of Organoelement Compounds RAS) for the performing of X-ray diffraction experiments and fruitful discussion, and Dr. Roman Borisov (Laboratory of Mass-spectrometry of A.V.Topchiev Institute of Petrochemical Synthesis RAS) for the performing of NALDI-TOF experiments. This work was partially supported by the Russian Fund for Basic Research (grant No. 12-0300839-A).

## Appendix A. Supplementary material

CCDC 917057 (**2a**) and No. 917058 (**2b**) contain the supplementary crystallographic data for this paper. These data can be obtained free of charge from The Cambridge Crystallographic Data Centre via www.ccdc.cam.ac.uk/data_request/cif Supplementary data associated with this article can be found, in the online version, at http://dx.doi.org/10.1016/j.ica.2014.02.013.

## References

[1] J. Kido, K. Nagai, Y. Ohashi, Org. Lett. 19 (1990) 657.
[2] J. Kido, Y. Okamoto, Chem. Rev. 102 (2002) 2357.
[3] M.A. Katkova, A.G. Vitukhnovsky, M.N. Bochkarev, Usp. Khim. 74 (2005) 1193.
[4] A. de Bettencourt-Dias, Dalton Trans. (2007) 2229.
[5] S. Comby, J.-C. G. Bunzli, Lanthanide near-infrared luminescence in molecular probes and devices, in: Handbook on the Physics and Chemistry of Rare Earths, vol. 37, Elsevier, 2007, p. 217.
[6] K. Binnemans, Chem. Rev. 109 (2009) 4283.
[7] V.A. Montes, R. Pohl, J. Shinar, P. Anzenbacher, Chem.-Eur. J. 12 (2006) 4523.
[8] M.A. Katkova, V.A. Ilichev, A.N. Konev, M.N. Bochkarev, A.G. Vitukhnovsky, M.A. Parshin, L. Pandey, M. Van der Auweraer, J. App. Phys. 104 (2008) 053706.
[9] M.A. Katkova, T.V. Balashova, V.A. Ilichev, A.N. Konev, N.A. Isachenkov, G.K. Fukin, S.Y. Ketkov, M.N. Bochkarev, Inorg. Chem. 49 (2010) 5094.
[10] W. Zhu, Q. Jiang, Z. Lu, X. Wei, M. Xie, D. Zou, T. Tsutsui, Thin Solid Films 363 (2000) 167.
[11] I.V. Taydakov, Pyrazol substituted 1.3-diketones: synthesis, complexing properties and application in rare earths coordination chemistry, in: Rare Earths: New Research, Nova Science Publishers, 2013, 95.
[12] I.V. Taydakov, S.S. Krasnoselskiy, Chem. Heterocycl. Compounds 47 (2011) 695.
[13] D. Rehder, Early Transition Metals, Plenum Press, Lanthanides and Actinides. Multinuclear NMR, 1987. 479.
[14] B. Stöger, P. Kaunty, D. Lumpi, E. Zobetz, J. Fröhlich, Acta Cryst. B68 (2012) 667.

[15] Bruker, Programs APEX II, version 2.0-1; SAINT, version 7.23A; SADABS, version 2004/1; XPREP, version 2005/2; SHELXTL, version 6.1, Bruker AXS Inc., Madison, WI, USA, 2005.
[16] G.M. Sheldrick, SHELXTL v. 5.10, Structure Determination Software Suite, Bruker AXS, Madison, Wisconsin, USA, 1998.
[17] A.L. Spek, J. Appl. Cryst. 36 (2003) 7.
[18] D.W. Bennett, T.A. Siddiquee, D.T. Haworth, S.V. Lindeman, J. Chem. Cryst. 37 (2007) 207.
[19] S.S. Krasnoselskiy, Synthesis and Study of Physical-chemical Properties of Complexes of Eu(III) and Tb(III) with β-Diketones Bearing Pyrazole Moiety (Ph.D. thesis), Peoples' Friendship University of Russia, 2013 (in Russ.).
[20] R. Knochenmuss, MALDI ionization mechanisms: an overview, in: Electrospray and MALDI Mass Spectrometry: Fundamentals, Instrumentation, Practicalities, and Biological Application, John Wiley & Sons, 2010, 149.